



Title	Confirmation of the X(1835) and observation of the resonances X(2120) and X(2370) in J/ + -
-------	---

Confirmation of the $X(1835)$ and Observation of the Resonances $X(2120)$ and $X(2370)$ in $J/\psi \rightarrow \gamma\pi^+\pi^-\eta'$

M. Ablikim,¹ M. N. Achasov,⁵ L. An,⁹ Q. An,³⁶ Z. H. An,¹ J. Z. Bai,¹ R. Baldini,¹⁷ Y. Ban,²³ J. Becker,² N. Berger,¹ M. Bertani,¹⁷ J. M. Bian,¹ I. Boyko,¹⁵ R. A. Briere,³ V. Bytev,¹⁵ X. Cai,¹ G. F. Cao,¹ X. X. Cao,¹ J. F. Chang,¹ G. Chelkov,^{15,*} G. Chen,¹ H. S. Chen,¹ J. C. Chen,¹ M. L. Chen,¹ S. J. Chen,²¹ Y. Chen,¹ Y. B. Chen,¹ H. P. Cheng,¹¹ Y. P. Chu,¹ D. Cronin-Hennessy,³⁵ H. L. Dai,¹ J. P. Dai,¹ D. Dedovich,¹⁵ Z. Y. Deng,¹ I. Denysenko,^{15,†} M. Destefanis,³⁸ Y. Ding,¹⁹ L. Y. Dong,¹ M. Y. Dong,¹ S. X. Du,⁴² M. Y. Duan,²⁶ R. R. Fan,¹ J. Fang,¹ S. S. Fang,¹ F. Feldbauer,² C. Q. Feng,³⁶ C. D. Fu,¹ J. L. Fu,²¹ Y. Gao,³² C. Geng,³⁶ K. Goetzen,⁷ W. X. Gong,¹ M. Greco,³⁸ S. Grishin,¹⁵ M. H. Gu,¹ Y. T. Gu,⁹ Y. H. Guan,⁶ A. Q. Guo,²² L. B. Guo,²⁰ Y. P. Guo,²² X. Q. Hao,¹ F. A. Harris,³⁴ K. L. He,¹ M. He,¹ Z. Y. He,²² Y. K. Heng,¹ Z. L. Hou,¹ H. M. Hu,¹ J. F. Hu,⁶ T. Hu,¹ B. Huang,¹ G. M. Huang,¹² J. S. Huang,¹⁰ X. T. Huang,²⁵ Y. P. Huang,¹ T. Hussain,³⁷ C. S. Ji,³⁶ Q. Ji,¹ X. B. Ji,¹ X. L. Ji,¹ L. K. Jia,¹ L. L. Jiang,¹ X. S. Jiang,¹ J. B. Jiao,²⁵ Z. Jiao,¹¹ D. P. Jin,¹ S. Jin,¹ F. F. Jing,³² M. Kavatsyuk,¹⁶ S. Komamiya,³¹ W. Kuehn,³³ J. S. Lange,³³ J. K. C. Leung,³⁰ Cheng Li,³⁶ Cui Li,³⁶ D. M. Li,⁴² F. Li,¹ G. Li,¹ H. B. Li,¹ J. C. Li,¹ Lei Li,¹ N. B. Li,²⁰ Q. J. Li,¹ W. D. Li,¹ W. G. Li,¹ X. L. Li,²⁵ X. N. Li,¹ X. Q. Li,²² X. R. Li,¹ Z. B. Li,²⁸ H. Liang,³⁶ Y. F. Liang,²⁷ Y. T. Liang,³³ G. R. Liao,⁸ X. T. Liao,¹ B. J. Liu,²⁹ B. J. Liu,³⁰ C. L. Liu,³ C. X. Liu,¹ C. Y. Liu,¹ F. H. Liu,²⁶ Fang Liu,¹ Feng Liu,¹² G. C. Liu,¹ H. Liu,¹ H. B. Liu,⁶ H. M. Liu,¹ H. W. Liu,¹ J. P. Liu,⁴⁰ K. Liu,²³ K. Y. Liu,¹⁹ Q. Liu,³⁴ S. B. Liu,³⁶ X. Liu,¹⁸ X. H. Liu,¹ Y. B. Liu,²² Y. W. Liu,³⁶ Yong Liu,¹ Z. A. Liu,¹ Z. Q. Liu,¹ H. Loehner,¹⁶ G. R. Lu,¹⁰ H. J. Lu,¹¹ J. G. Lu,¹ Q. W. Lu,²⁶ X. R. Lu,⁶ Y. P. Lu,¹ C. L. Luo,²⁰ M. X. Luo,⁴¹ T. Luo,¹ X. L. Luo,¹ C. L. Ma,⁶ F. C. Ma,¹⁹ H. L. Ma,¹ Q. M. Ma,¹ T. Ma,¹ X. Ma,¹ X. Y. Ma,¹ M. Maggiora,³⁸ Q. A. Malik,³⁷ H. Mao,¹ Y. J. Mao,²³ Z. P. Mao,¹ J. G. Messchendorp,¹⁶ J. Min,¹ R. E. Mitchell,¹⁴ X. H. Mo,¹ C. Motzko,² N. Yu. Muchnoi,⁵ Y. Nefedov,¹⁵ Z. Ning,¹ S. L. Olsen,²⁴ Q. Ouyang,¹⁷ S. Pacetti,¹⁷ M. Pelizaeus,³⁴ K. Peters,⁷ J. L. Ping,²⁰ R. G. Ping,¹ R. Poling,³⁵ C. S. J. Pun,³⁰ M. Qi,²¹ S. Qian,¹ C. F. Qiao,⁶ X. S. Qin,¹ J. F. Qiu,¹ K. H. Rashid,³⁷ G. Rong,¹ X. D. Ruan,⁹ A. Sarantsev,^{15,‡} J. Schulze,² M. Shao,³⁶ C. P. Shen,³⁴ X. Y. Shen,¹ H. Y. Sheng,¹ M. R. Shepherd,¹⁴ X. Y. Song,¹ S. Sonoda,³¹ S. Spataro,³⁸ B. Spruck,³³ D. H. Sun,¹ G. X. Sun,¹ J. F. Sun,¹⁰ S. S. Sun,¹ X. D. Sun,¹ Y. J. Sun,³⁶ Y. Z. Sun,¹ Z. J. Sun,¹ Z. T. Sun,³⁶ C. J. Tang,²⁷ X. Tang,¹ X. F. Tang,⁸ H. L. Tian,¹ D. Toth,³⁵ G. S. Varner,³⁴ X. Wan,¹ B. Q. Wang,²³ K. Wang,¹ L. L. Wang,⁴ L. S. Wang,¹ M. Wang,²⁵ P. Wang,¹ P. L. Wang,¹ Q. Wang,¹ S. G. Wang,²³ X. L. Wang,³⁶ Y. D. Wang,³⁶ Y. F. Wang,¹ Y. Q. Wang,²⁵ Z. Wang,¹ Z. G. Wang,¹ Z. Y. Wang,¹ D. H. Wei,⁸ S. P. Wen,¹ U. Wiedner,² L. H. Wu,¹ N. Wu,¹ W. Wu,¹⁹ Z. Wu,¹ Z. J. Xiao,²⁰ Y. G. Xie,¹ G. F. Xu,¹ G. M. Xu,²³ H. Xu,¹ Y. Xu,²² Z. R. Xu,³⁶ Z. Z. Xu,³⁶ Z. Xue,¹ L. Yan,³⁶ W. B. Yan,³⁶ Y. H. Yan,¹³ H. X. Yang,¹ M. Yang,¹ T. Yang,⁹ Y. Yang,¹² Y. X. Yang,⁸ M. Ye,¹ M. H. Ye,⁴ B. X. Yu,¹ C. X. Yu,²² L. Yu,¹² C. Z. Yuan,¹ W. L. Yuan,²⁰ Y. Yuan,¹ A. A. Zafar,³⁷ A. Zallo,¹⁷ Y. Zeng,¹³ B. X. Zhang,¹ B. Y. Zhang,¹ C. C. Zhang,¹ D. H. Zhang,¹ H. H. Zhang,²⁸ H. Y. Zhang,¹ J. Zhang,²⁰ J. W. Zhang,¹ J. Y. Zhang,¹ J. Z. Zhang,¹ L. Zhang,²¹ S. H. Zhang,¹ T. R. Zhang,²⁰ X. J. Zhang,¹ X. Y. Zhang,²⁵ Y. Zhang,¹ Y. H. Zhang,¹ Z. P. Zhang,³⁶ Z. Y. Zhang,⁴⁰ G. Zhao,¹ H. S. Zhao,¹ Jiawei Zhao,³⁶ Jingwei Zhao,¹ Lei Zhao,³⁶ Ling Zhao,¹ M. G. Zhao,²² Q. Zhao,¹ S. J. Zhao,⁴² T. C. Zhao,³⁹ X. H. Zhao,²¹ Y. B. Zhao,¹ Z. G. Zhao,³⁶ Z. L. Zhao,⁹ A. Zhemchugov,^{15,*} B. Zheng,¹ J. P. Zheng,¹ Y. H. Zheng,⁶ Z. P. Zheng,¹ B. Zhong,¹ J. Zhong,² L. Zhong,³² L. Zhou,¹ X. K. Zhou,⁶ X. R. Zhou,³⁶ C. Zhu,¹ K. Zhu,¹ K. J. Zhu,¹ S. H. Zhu,¹ X. L. Zhu,³² X. W. Zhu,¹ Y. S. Zhu,¹ Z. A. Zhu,¹ J. Zhuang,¹ B. S. Zou,¹ J. H. Zou,¹ J. X. Zuo,¹ and P. Zveber³⁵

(BESIII Collaboration)

¹*Institute of High Energy Physics, Beijing 100049, P. R. China*

²*Bochum Ruhr-University, 44780 Bochum, Germany*

³*Carnegie Mellon University, Pittsburgh, Pennsylvania 15213, USA*

⁴*China Center of Advanced Science and Technology, Beijing 100190, People's Republic of China*

⁵*G.I. Budker Institute of Nuclear Physics SB RAS (BINP), Novosibirsk 630090, Russia*

⁶*Graduate University of Chinese Academy of Sciences, Beijing 100049, People's Republic of China*

⁷*GSI Helmholtzcentre for Heavy Ion Research GmbH, D-64291 Darmstadt, Germany*

⁸*Guangxi Normal University, Guilin 541004, People's Republic of China*

⁹*Guangxi University, Nanning 530004, People's Republic of China*

¹⁰*Henan Normal University, Xinxiang 453007, People's Republic of China*

¹¹*Huangshan College, Huangshan 245000, People's Republic of China*

¹²*Huazhong Normal University, Wuhan 430079, People's Republic of China*

- ¹³Hunan University, Changsha 410082, People's Republic of China
¹⁴Indiana University, Bloomington, Indiana 47405, USA
¹⁵Joint Institute for Nuclear Research, 141980 Dubna, Russia
¹⁶KVI/University of Groningen, 9747 AA Groningen, The Netherlands
¹⁷Laboratori Nazionali di Frascati-INFN, 00044 Frascati, Italy
¹⁸Lanzhou University, Lanzhou 730000, People's Republic of China
¹⁹Liaoning University, Shenyang 110036, People's Republic of China
²⁰Nanjing Normal University, Nanjing 210046, People's Republic of China
²¹Nanjing University, Nanjing 210093, People's Republic of China
²²Nankai University, Tianjin 300071, People's Republic of China
²³Peking University, Beijing 100871, People's Republic of China
²⁴Seoul National University, Seoul, 151-747 Korea
²⁵Shandong University, Jinan 250100, People's Republic of China
²⁶Shanxi University, Taiyuan 030006, People's Republic of China
²⁷Sichuan University, Chengdu 610064, People's Republic of China
²⁸Sun Yat-Sen University, Guangzhou 510275, People's Republic of China
²⁹The Chinese University of Hong Kong, Shatin, N.T., Hong Kong
³⁰The University of Hong Kong, Pokfulam, Hong Kong
³¹The University of Tokyo, Tokyo 113-0033 Japan
³²Tsinghua University, Beijing 100084, People's Republic of China
³³Universitaet Giessen, 35392 Giessen, Germany
³⁴University of Hawaii, Honolulu, Hawaii 96822, USA
³⁵University of Minnesota, Minneapolis, Minnesota 55455, USA
³⁶University of Science and Technology of China, Hefei 230026, People's Republic of China
³⁷University of the Punjab, Lahore-54590, Pakistan
³⁸University of Turin and INFN, Turin, Italy
³⁹University of Washington, Seattle, Washington 98195, USA
⁴⁰Wuhan University, Wuhan 430072, People's Republic of China
⁴¹Zhejiang University, Hangzhou 310027, People's Republic of China
⁴²Zhengzhou University, Zhengzhou 450001, People's Republic of China
(Received 16 December 2010; published 16 February 2011)

With a sample of $(225.2 \pm 2.8) \times 10^6$ J/ψ events registered in the BESIII detector, $J/\psi \rightarrow \gamma\pi^+\pi^-\eta'$ is studied using two η' decay modes: $\eta' \rightarrow \pi^+\pi^-\eta$ and $\eta' \rightarrow \gamma\rho^0$. The $X(1835)$, which was previously observed by BESII, is confirmed with a statistical significance that is larger than 20σ . In addition, in the $\pi^+\pi^-\eta'$ invariant-mass spectrum, the $X(2120)$ and the $X(2370)$, are observed with statistical significances larger than 7.2σ and 6.4σ , respectively. For the $X(1835)$, the angular distribution of the radiative photon is consistent with expectations for a pseudoscalar.

DOI: 10.1103/PhysRevLett.106.072002

PACS numbers: 12.39.Mk, 12.40.Yx, 13.20.Gd, 13.75.Cs

A $\pi^+\pi^-\eta'$ resonance, the $X(1835)$, was observed in $J/\psi \rightarrow \gamma\pi^+\pi^-\eta'$ decays with a statistical significance of 7.7σ by the BESII experiment [1]. A fit to a Breit-Wigner function yielded a mass $M = 1833.7 \pm 6.1(\text{stat}) \pm 2.7(\text{syst})$ MeV/ c^2 , a width $\Gamma = 67.7 \pm 20.3(\text{stat}) \pm 7.7(\text{syst})$ MeV/ c^2 , and a product branching fraction $B(J/\psi \rightarrow \gamma X) \cdot B(X \rightarrow \pi^+\pi^-\eta') = [2.2 \pm 0.4(\text{stat}) \pm 0.4(\text{syst})] \times 10^{-4}$. The study was stimulated by the anomalous $p\bar{p}$ invariance mass threshold enhancement, that was reported in $J/\psi \rightarrow \gamma p\bar{p}$ decays by the BESII experiment [2] and was recently confirmed in an analysis of $\psi' \rightarrow \pi^+\pi^-J/\psi$, $J/\psi \rightarrow \gamma p\bar{p}$ decays by the BESIII experiment [3]. The possible interpretations of the $X(1835)$ include a $p\bar{p}$ bound state [4–7], a glueball [8–10], a radial excitation of the η' meson [11], etc. A high statistics data sample collected with BESIII provides an opportunity to confirm the existence of the $X(1835)$ and look for possible related states that decay to $\pi^+\pi^-\eta'$, and the study of such states may help us to understand the dynamics of QCD.

Lattice QCD predicts that the lowest lying pseudoscalar glueball meson has a mass that is around 2.3 GeV/ c^2 [12]. This pseudoscalar glueball may have properties in common with the η_c , due to its similar decay dynamics that favor decays into gluons. One of the strongest decay channels of the η_c is $\pi^+\pi^-\eta'$. Thus $J/\psi \rightarrow \gamma\pi^+\pi^-\eta'$ decays may be a good channel for finding 0^{-+} glueballs.

In this Letter, we report a study of $J/\psi \rightarrow \gamma\pi^+\pi^-\eta'$ that uses two η' decay modes, $\eta' \rightarrow \gamma\rho$ and $\eta' \rightarrow \pi^+\pi^-\eta$. The analysis uses a sample of $(225.2 \pm 2.8) \times 10^6$ J/ψ events [13] accumulated in the new Beijing Spectrometer (BESIII) [14] located at the Beijing Electron-Positron Collider (BEPCII) [15] at the Beijing Institute of High Energy Physics.

BEPCII is a two-ring e^+e^- collider designed for a peak luminosity of 10^{33} cm $^{-2}$ s $^{-1}$ at a beam current of 0.93 A. The cylindrical core of the BESIII detector consists of a helium-gas-based drift chamber, a plastic scintillator time-of-flight system (TOF), and a CsI(Tl) electromagnetic

calorimeter, all enclosed in a superconducting solenoidal magnet providing a 1.0-T magnetic field. The solenoid is supported by an octagonal flux-return yoke with resistive plate counter muon identifier modules interleaved with steel. The charged particle and photon acceptance is 93% of 4π , and the charged particle momentum and photon energy resolutions at 1 GeV are 0.5% and 2.5%, respectively. The time resolution of TOF is 80 ps in the barrel and 110 ps in the endcaps, and the dE/dx resolution is 6%.

Charged-particle tracks in the polar angle range $|\cos\theta| < 0.93$ are reconstructed from hits in the helium-gas-based drift chamber. Tracks that extrapolate to be within 20 cm of the interaction point in the beam direction and 2 cm in the plane perpendicular to the beam are selected. The TOF and dE/dx information are combined to form particle identification confidence levels for the π , K , and p hypotheses; each track is assigned to the particle type that corresponds to the hypothesis with the highest confidence level. Photon candidates are required to have at least 100 MeV of energy in the electromagnetic calorimeter regions $|\cos\theta| < 0.8$ and $0.86 < |\cos\theta| < 0.92$ and be isolated from all charged tracks by more than 5° . In this analysis, candidate events are required to have four charged tracks (zero net charge) with at least three of the charged tracks identified as pions. At least two photons (three photons) are required for the $\eta' \rightarrow \gamma\rho$ ($\eta' \rightarrow \pi^+\pi^-\eta$) channel.

For $J/\psi \rightarrow \gamma\pi^+\pi^-\eta'$ ($\eta' \rightarrow \gamma\rho$), a four-constraint (4C) energy-momentum conservation kinematic fit is performed to the $\gamma\gamma\pi^+\pi^-\pi^+\pi^-$ hypothesis. For events with more than two photon candidates, the combination with the minimum χ^2 is used, and $\chi^2_{4C} < 40$ is required. Events with $|M_{\gamma\gamma} - m_{\pi^0}| < 0.04$ GeV/ c^2 , $|M_{\gamma\gamma} - m_\eta| < 0.03$ GeV/ c^2 , 0.72 GeV/ $c^2 < M_{\gamma\gamma} < 0.82$ GeV/ c^2 , or $|M_{\gamma\pi^+\pi^-} - m_\eta| < 0.007$ GeV/ c^2 are rejected to suppress the background from $\pi^0\pi^+\pi^-\pi^+\pi^-$, $\eta\pi^+\pi^-\pi^+\pi^-$, $\omega(\omega \rightarrow \gamma\pi^0)\pi^+\pi^-\pi^+\pi^-$, and $\gamma\pi^+\pi^-\eta(\eta \rightarrow \gamma\pi^+\pi^-)$, respectively. A clear η' signal with a 5 MeV/ c^2 mass resolution is evident in the mass spectrum of all selected $\gamma\pi^+\pi^-$ combinations shown in Fig. 1(a). Candidate ρ and η' mesons are reconstructed from the $\pi^+\pi^-$ and $\gamma\pi^+\pi^-$ pairs with $|M_{\pi^+\pi^-} - m_\rho| < 0.2$ GeV/ c^2 and $|M_{\gamma\pi^+\pi^-} - m_{\eta'}| < 0.015$ GeV/ c^2 , respectively. If more than one combination passes these criteria, the combination with $M_{\gamma\pi^+\pi^-}$ closest to $m_{\eta'}$ is selected. After the above selection, the $X(1835)$ resonance is clearly visible in the $\pi^+\pi^-\eta'$ invariant-mass spectrum of Fig. 1(b). Also, additional peaks are evident around 2.1 and 2.4 GeV/ c^2 as well as a distinct signal for the η_c .

For $J/\psi \rightarrow \gamma\pi^+\pi^-\eta'$ ($\eta' \rightarrow \pi^+\pi^-\eta$), a 4C kinematic fit to the $\gamma\gamma\pi^+\pi^-\pi^+\pi^-$ hypothesis is performed. If there are more than three photon candidates, the combination with the minimum χ^2_{4C} is selected, and $\chi^2_{4C} < 40$ is required. In order to reduce the combinatorial background events from $\pi^0 \rightarrow \gamma\gamma$, $|M_{\gamma\gamma} - m_{\pi^0}| > 0.04$ GeV/ c^2 is required for all photon pairs. The η candidates are selected

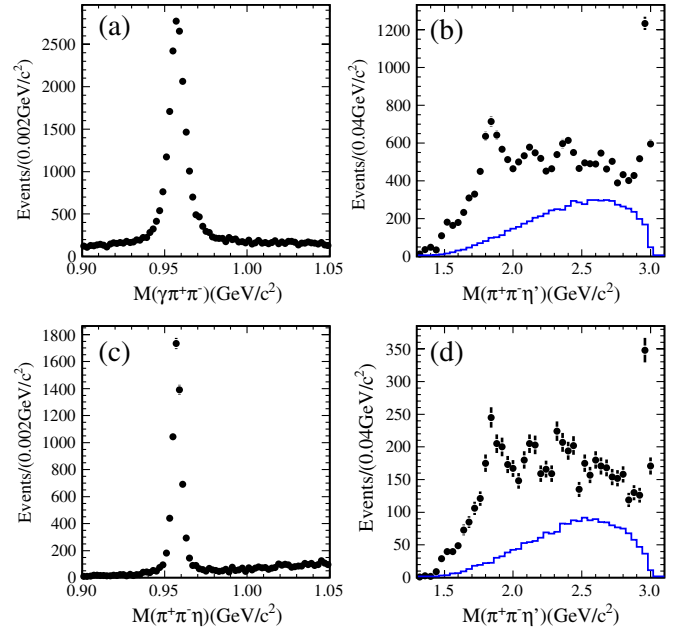


FIG. 1 (color online). Invariant-mass distributions for the selected candidate events. Panels (a) and (b) are the $\gamma\pi^+\pi^-$ invariant-mass spectrum and the $\pi^+\pi^-\eta'$ invariant-mass spectrum for $\eta' \rightarrow \gamma\rho$, respectively. Panels (c) and (d) are the $\pi^+\pi^-\eta$ invariant-mass spectrum and the $\pi^+\pi^-\eta'$ invariant-mass spectrum for $\eta' \rightarrow \pi^+\pi^-\eta$, respectively. The histograms in (b) and (d) are from $J/\psi \rightarrow \gamma\pi^+\pi^-\eta'$ phase-space MC events (with arbitrary normalization) for $\eta' \rightarrow \gamma\rho$ and $\eta' \rightarrow \pi^+\pi^-\eta$, respectively.

by requiring $|M_{\gamma\gamma} - m_\eta| < 0.03$ GeV/ c^2 . A five-constraint fit with an η mass constraint is used to improve the mass resolution from 8 MeV/ c^2 (4C) to 3 MeV/ c^2 , as shown in Fig. 1(c) where $\chi^2_{5C} < 40$ is required. To select η' mesons, $|M_{\pi^+\pi^-\eta} - m_{\eta'}| < 0.01$ GeV/ c^2 is required. If more than one combination passes the above selection, the combination with $M_{\pi^+\pi^-\eta}$ closest to $m_{\eta'}$ is selected. After the above selection, structures similar to those seen for the $\eta' \rightarrow \gamma\rho$ channel in the $\pi^+\pi^-\eta'$ invariant-mass spectrum can be seen in Fig. 1(d), namely, peaks near 1.8, 2.1, and 2.4 GeV/ c^2 as well as the η_c .

Potential background processes are studied with an inclusive sample of 2×10^8 J/ψ events generated according to the Lund-Charm model [16] and the Particle Data Group (PDG) decay tables [17]. There are no peaking backgrounds at the positions of the three resonances. To ensure further that the three peaks are not due to background, we have studied potential exclusive background processes using data. The main background channel is from $J/\psi \rightarrow \pi^0\pi^+\pi^-\eta'$. Non- η' processes are studied with η' mass-sideband events. Neither of these produce peaking structures.

The $\pi^+\pi^-\eta'$ invariant-mass spectrum for the combined two η' decay modes is presented in Fig. 2. Here a small peak at the position of the $f_1(1510)$ signal is also present. Fits to the mass spectra have been made using four

efficiency-corrected Breit-Wigner functions convolved with a Gaussian mass resolution plus a nonresonant $\pi^+\pi^-\eta'$ contribution and background representations, where the efficiency for the combined channels is obtained from the branching-ratio-weighted average of the efficiencies for the two η' modes. The contribution from nonresonant $\gamma\pi^+\pi^-\eta'$ production is described by reconstructed Monte Carlo (MC)-generated $J/\psi \rightarrow \gamma\pi^+\pi^-\eta'$ phase space decays, and it is treated as an incoherent process. The background contribution can be divided into two different components: the contribution from non- η' events estimated from η' mass sideband, and the contribution from $J/\psi \rightarrow \pi^0\pi^+\pi^-\eta'$. For the second background, we obtain the background $\pi^+\pi^-\eta'$ mass spectrum from data by selecting $J/\psi \rightarrow \pi^0\pi^+\pi^-\eta'$ events and reweighting their mass spectrum with a weight equal to the MC efficiency ratio of the $\gamma\pi^+\pi^-\eta'$ and $\pi^0\pi^+\pi^-\eta'$ selections for $J/\psi \rightarrow \pi^0\pi^+\pi^-\eta'$. The masses, widths, and number of events of the $f_1(1510)$, the $X(1835)$ and the resonances near 2.1 and 2.4 GeV/ c^2 , the $X(2120)$ and $X(2370)$, are listed in Table I. The statistical significance is determined from the change in $-2\ln L$ in the fits to mass spectra with and without signal assumption while considering the change of degree of freedom of the fits. With the systematic uncertainties in the fit taken into account, the statistical

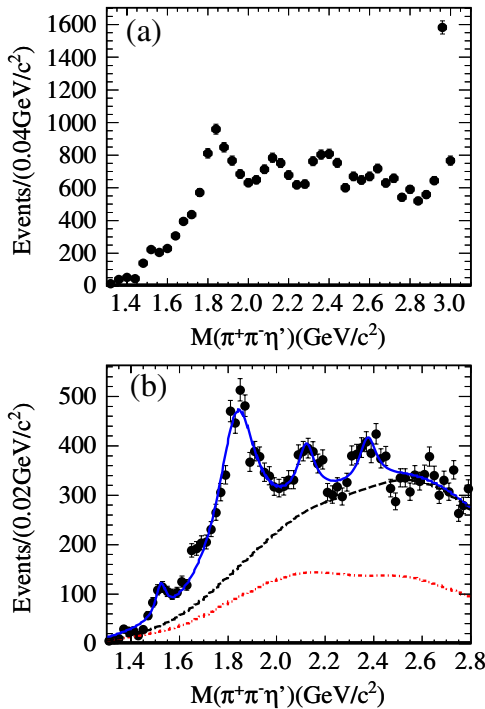


FIG. 2 (color online). (a) The $\pi^+\pi^-\eta'$ invariant-mass distribution for the selected events from the two η' decay modes. (b) Mass spectrum fitting with four resonances; here, the dash-dotted line is contributions of non- η' events and the $\pi^0\pi^+\pi^-\eta'$ background for two η' decay modes, and the dashed line is contributions of the total background and nonresonant $\pi^+\pi^-\eta'$ process.

TABLE I. Fit results with four resonances for the combined two η' decay modes

Resonance	$M(\text{MeV}/c^2)$	$\Gamma(\text{MeV}/c^2)$	N_{event}
$f_1(1510)$	1522.7 ± 5.0	48 ± 11	230 ± 37
$X(1835)$	1836.5 ± 3.0	190.1 ± 9.0	4265 ± 131
$X(2120)$	2122.4 ± 6.7	83 ± 16	647 ± 103
$X(2370)$	2376.3 ± 8.7	83 ± 17	565 ± 105

significance of the $X(1835)$ is larger than 20σ , while those for the $f_1(1510)$, the $X(2120)$, and the $X(2370)$ are larger than 5.7σ , 7.2σ , and 6.4σ , respectively. The mass and width from the fit of the $f_1(1510)$ are consistent with PDG values [17]. With MC-determined selection efficiencies of 16.0% and 11.3% for the $\eta' \rightarrow \gamma\rho$ and $\eta' \rightarrow \pi^+\pi^-\eta$ decay modes, respectively, the branching fraction for the $X(1835)$ is measured to be $B(J/\psi \rightarrow \gamma X(1835)) B(X(1835) \rightarrow \pi^+\pi^-\eta') = (2.87 \pm 0.09) \times 10^{-4}$. The consistency between the two η' decay modes is checked by fitting their $\pi^+\pi^-\eta'$ mass distribution separately with the procedure described above.

For radiative J/ψ decays to a pseudoscalar meson, the polar angle of the photon in the J/ψ center of mass system, θ_γ , should be distributed according to $1 + \cos^2\theta_\gamma$. We divide the $|\cos\theta_\gamma|$ distribution into 10 bins in the region of $[0, 1, 0]$. With the same procedure as described above, the number of the $X(1835)$ events in each bin can be obtained by fitting the mass spectrum in this bin, and then the background-subtracted, acceptance-corrected $|\cos\theta_\gamma|$ distribution for the $X(1835)$ is obtained as shown in Fig. 3, where the errors are statistical only. It agrees with $1 + \cos^2\theta_\gamma$, which is expected for a pseudoscalar, with $\chi^2/\text{d.o.f} = 11.8/9$.

The systematic uncertainties on the mass and width are mainly from the uncertainty of background representation, the mass range included in the fit, different shapes for background contributions, and the nonresonant process and contributions of possible additional resonances in the 1.6 GeV/ c^2 and 2.6 GeV/ c^2 mass regions. The total systematic errors on the mass and width are $^{+5.6}_{-2.1}$ and

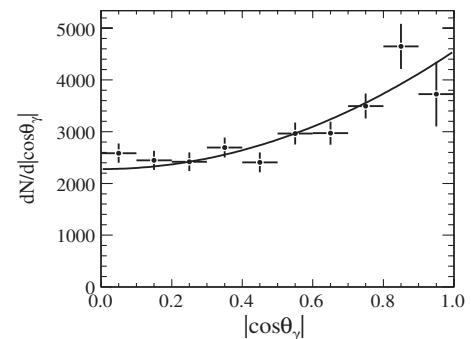


FIG. 3. The background-subtracted, acceptance-corrected $|\cos\theta_\gamma|$ distribution of the $X(1835)$ for two η' decay modes for $J/\psi \rightarrow \gamma\pi^+\pi^-\eta'$.

$^{+38}_{-36}$ MeV/ c^2 for the $X(1835)$, $^{+4.7}_{-2.7}$ and $^{+31}_{-11}$ MeV/ c^2 for the $X(2120)$, $^{+3.2}_{-4.3}$ and $^{+44}_{-6}$ MeV/ c^2 for the $X(2370)$, respectively. For the systematic error of the branching fraction measurement, we additionally include the uncertainties of the MC generator, charged track detection efficiency, particle identification efficiency, photon detection efficiency, kinematic fit, the η' decay branching fractions to $\pi^+\pi^-\eta$ and $\gamma\rho$ [17], the requirement on the $\gamma\gamma$ invariant-mass distribution, signals selection of ρ , η , and η' and the total number of J/ψ events [13]. The main contribution also comes from the uncertainty in the background estimation, and the total relative systematic error on the product branching fraction for the $X(1835)$ is $^{+17\%}_{-18\%}$.

In summary, the decay channel $J/\psi \rightarrow \pi^+\pi^-\eta'$ is analyzed using two η' decay modes, $\eta' \rightarrow \gamma\rho$ and $\eta' \rightarrow \pi^+\pi^-\eta$. The $X(1835)$, which was first observed at BESII, has been confirmed with a statistical significance larger than 20σ . Meanwhile, two resonances, the $X(2120)$ and the $X(2370)$ are observed with statistical significances larger than 7.2σ and 6.4σ , respectively. The masses and widths are measured to be

$X(1835)$

$$M = 1836.5 \pm 3.0(\text{stat})^{+5.6}_{-2.1}(\text{syst}) \text{ MeV}/c^2$$

$$\Gamma = 190 \pm 9(\text{stat})^{+38}_{-36}(\text{syst}) \text{ MeV}/c^2$$

$X(2120)$

$$M = 2122.4 \pm 6.7(\text{stat})^{+4.7}_{-2.7}(\text{syst}) \text{ MeV}/c^2$$

$$\Gamma = 83 \pm 16(\text{stat})^{+31}_{-11}(\text{syst}) \text{ MeV}/c^2$$

$X(2370)$

$$M = 2376.3 \pm 8.7(\text{stat})^{+3.2}_{-4.3}(\text{syst}) \text{ MeV}/c^2$$

$$\Gamma = 83 \pm 17(\text{stat})^{+44}_{-6}(\text{syst}) \text{ MeV}/c^2.$$

For the $X(1835)$, the product branching fraction is $B[J/\psi \rightarrow \gamma X(1835)] \cdot B(X(1835) \rightarrow \pi^+\pi^-\eta') = [2.87 \pm 0.09(\text{stat})^{+0.49}_{-0.52}(\text{syst})] \times 10^{-4}$, and the angular distribution of the radiative photon is consistent with a pseudoscalar assignment. The mass of the $X(1835)$ is consistent with the BESII result, but the width is significantly larger. If we fit the mass spectrum with one resonance as BESII, the mass and width of the $X(1835)$ are 1841.2 ± 2.9 MeV/ c^2 and 109 ± 11 MeV/ c^2 , where the errors are statistical only.

In the mass spectrum fitting in Fig. 2(b), possible interferences among different resonances and the nonresonant process are not taken into account which might be a source of the large χ^2 value for the fit ($\chi^2/\text{d.o.f} = 144/62$). The dips around 2.2 GeV/ c^2 and 2.5 GeV/ c^2 may not be fitted well due to the neglect of such interferences. In the absence of knowledge of the spin parities of the resonances and their decay intermediate states, reliable fits that include interference cannot be done.

It is intriguing that it is the first time resonant structures are observed in the 2.3 GeV/ c^2 region in the $\pi^+\pi^-\eta'$

mode and in J/ψ radiative decays which a 0^{-+} glueball may favor to decay to and to be produced from. To understand the nature of the $X(1835)$, $X(2120)$, and $X(2370)$, it would be crucial to measure their spin parities and to search for them in more decay modes and in more production mechanisms. To determine their spin parities, and to measure their masses and widths more precisely, a partial wave analysis must be performed, which will be possible with the much higher statistics J/ψ data samples planned for future runs of the BESIII experiment.

We thank the accelerator group and computer staff of IHEP for their effort in producing beams and processing data. We are grateful for support from our institutes and universities and from these agencies: Ministry of Science and Technology of China, National Natural Science Foundation of China, Chinese Academy of Sciences, Istituto Nazionale di Fisica Nucleare, Russian Foundation for Basic Research, Russian Academy of Science (Siberian branch), U.S. Department of Energy, and National Research Foundation of Korea.

*Also at the Moscow Institute of Physics and Technology, Moscow, Russia

†On leave from the Bogolyubov Institute for Theoretical Physics, Kiev, Ukraine

‡Also at the PNPI, Gatchina, Russia

- [1] M. Ablikim *et al.* (BES Collaboration), *Phys. Rev. Lett.* **95**, 262001 (2005).
- [2] J.Z. Bai *et al.* (BES Collaboration), *Phys. Rev. Lett.* **91**, 022001 (2003).
- [3] M. Ablikim *et al.* (BESIII Collaboration), *Chinese Phys. C* **34**, 421 (2010).
- [4] G.J. Ding and M.L. Yan, *Phys. Rev. C* **72**, 015208 (2005); G.J. Ding and M.L. Yan, *Eur. Phys. J. A* **28**, 351 (2006).
- [5] J.P. Dedonder *et al.*, *Phys. Rev. C* **80**, 045207 (2009).
- [6] C. Liu, *Eur. Phys. J. C* **53**, 413 (2007).
- [7] Z.G. Wang and S.L. Wan, *J. Phys. G* **34**, 505 (2007).
- [8] G. Hao, C.F. Qiao, and A.L. Zhang, *Phys. Lett. B* **642**, 53 (2006).
- [9] B.A. Li, *Phys. Rev. D* **74**, 034019 (2006).
- [10] N. Kochelev and D.P. Min, *Phys. Lett. B* **633**, 283 (2006).
- [11] T. Huang and S.L. Zhu, *Phys. Rev. D* **73**, 014023 (2006).
- [12] C. Amsler and N.A. Tornqvist, *Phys. Rev.* **389**, 61 (2004); E. Klempt and A. Zaitsev, *Phys. Rep.* **454**, 1 (2007); Y. Chen *et al.*, *Phys. Rev. D* **73**, 014516 (2006).
- [13] M. Ablikim *et al.* (BESIII Collaboration), *Phys. Rev. D* **83**, 012003 (2011).
- [14] M. Ablikim *et al.* (BESIII Collaboration), *Nucl. Instrum. Methods Phys. Res., Sect. A* **614**, 345 (2010).
- [15] J.Z. Bai *et al.* (BES Collaboration), *Nucl. Instrum. Methods Phys. Res., Sect. A* **344**, 319 (1994); *Nucl. Instrum. Methods Phys. Res., Sect. A* **458**, 627 (2001).
- [16] J.C. Chen *et al.*, *Phys. Rev. D* **62**, 034003 (2000).
- [17] K. Nakamura *et al.* (Particle Data Group), *J. Phys. G* **37**, 075021 (2010).